Proceedings of the 6th WSEAS International Conference on Robotics, Control and Manufacturing Technology, Hangzhou, China, April 16-18, 2006 (pp30-35)

Simulation and Analysis of Surface Generation in Micro-milling

YAZHOU SUN[1, 2] YINGCHUN LIANG[1] RUXU DU[2]

[1] School of Mechatronics Engineering
Harbin Institute of Technology
P.O.Box422, No.92, West Da-Zhi Street, Harbin, 150001
P. R. CHINA

[2] Department of Automation & Computer-Aided Engineering
The Chinese University of Hong Kong
Shatin, N. T.
HONG KONG, CHINA

Abstract: Micro-milling is a flexible and economical mean for manufacturing precision miniature components with three-dimensional geometry features in a wide range of materials. In this paper, a 2D model of surface generation is proposed based on the minimum cutting thickness. Through simulating the surface topography and computing the arithmetic surface roughness, R_a, the relationship among the surface roughness, the feed per tooth, as well as the cutter geometry is obtained. The model is validated by means of experiments.

Keywords: Micro-milling, Surface generation, Surface roughness, Minimum cutting thickness, Feed per tooth, Cutter geometry.

1 Introduction

The miniaturization of devices demands the manufacture of accurate miniature components with three-dimensional (3D) geometries with a wide range of materials. Presently, MEMS technologies such as photolithography and chemical etching, are the principal methods for producing these micro-scale miniature components, but they are not able to produce the components that have 3D geometry features. In recent years, micro-milling emerges as one of the primary technologies due to their inherent flexibility and economy [1-4]. However, it differs from conventional milling. For conventional milling, the surface generation models can accurately predict the surface topography [5, 6]. For micro-milling, the conventional surface generation model does not work very well [2-4]. In the conventional milling, the feed per tooth usually dominates the surface finish. In micro-milling, on the other hand, the feed per tooth is about the same size as that of the cutter radius. As a result, the actual rake angle becomes negative so that the rubbing and the plowing processes dominate. In order words, the cutter radius plays an equally important role. This results in the minimum cutting thickness effect [7, 8], beyond which, no chip is formed [3, 4].

Supported by the Scientific Research Foundation of Harbin Institute of Technology (HIT.2002.25) and the Hong Kong Innovation and Technology Commission (ITS/001/05)

This paper presents a new surface generation model for micro-milling. The rest of the paper is organized as follows: Firstly, in Section 2, a 2D model of surface generation is proposed. Secondly, Section 3 presents the experiment results of slot milling using our custom made miniature machine tool with a miniature flat end milling cutter. The experiment results match that of the simulation. In Section 4, using the model, the influences of the minimum cutting thickness, the feed per tooth and the geometry of the cutter are analyzed. Finally, Section 5 contains conclusions.

2 Modeling of Surface Generation in Micro-milling

2.1 Simulation model of surface generation

Considering a slot milling operation using a flat end milling cutter, as shown in Fig. 1, the cutting thickness, h_D, can be approximated as follows [9]:

$$h_{\mathrm{D}} = f_Z \sin\theta \tag{1}$$

where, f_z is the feed per tooth and θ the angular position of the tooth.

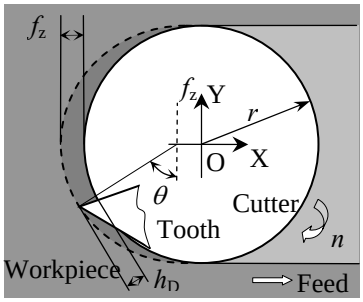

Fig.1 Schematic of the slot milling process

With each pass of the tooth, the surface generation process along the centerline of the slot floor, where θ is at 90°, can be described as follows: First, define the cutter geometry and the local coordinate system, *x*-*y*, as shown in Fig. 2(a). In the figure, the thick solid line represents the cutter profile with r_ε be the nose radius, and κ' the concave angle. Suppose that the cutting edge radius is r_n, the corresponding minimum cutting thickness is h_{Dmin}. The relationship between h_{Dmin} and r_n can be approximated as follows [7, 8]:

$$h_{\mathrm{Dmin}} = k \cdot r_{\mathrm{n}} \tag{2}$$

where, k is the ratio of the minimum cutting thickness to the cutting edge radius, which depends on material property, and usually ranges from 0.2 to 0.4. Then, all points along the cutter profile is shifted a distance h_{Dmin} along the normal direction, and then the corresponding line representing the minimum cutting thickness with the dashed is determined in Fig.2(b). For each pass of the tooth, the surface profile along the centerline of the slot floor is generated by the motion trajectories of the end cutting edge and the nose arc cutting edge. Then, the cutter profile y representing the end cutting edge and the nose arc cutting edge can be expressed as:

$$y = \begin{cases} \sqrt{r_\varepsilon^2 - x^2} & ; r_\varepsilon \geq x > -r_\varepsilon \sin\kappa' \\ r_\varepsilon \cos\kappa' + (x + r_\varepsilon \sin\kappa')\tan\kappa' ; x \leq -r_\varepsilon \sin\kappa' \end{cases} \tag{3}$$

The corresponding minimum cutting thickness profile y_{min} can be expressed as:

$$y_{\min} = \begin{cases} (r_\varepsilon - h_{\mathrm{Dmin}})\, y / r_\varepsilon , r_\varepsilon \geq x > -r_\varepsilon \sin\kappa' \\ y - h_{\mathrm{Dmin}} \cos\kappa', x \leq -r_\varepsilon \sin\kappa' \end{cases} \tag{4}$$

Suppose that the initial surface profile y_0 has the cutter profile y of equation (3), as shown in Fig.2(c), then, for the subsequent first tooth pass, the cutter profile y_1 can be expressed as:

$$y_1 = \begin{cases} \sqrt{r_\varepsilon^2 - (x - f_z)^2} & ; (r_\varepsilon + f_z) \geq x > (f_z - r_\varepsilon \sin\kappa') \\ r_\varepsilon \cos\kappa' + [(x - f_z) + r_\varepsilon \sin\kappa']\tan\kappa' ; x \leq (f_z - r_\varepsilon \sin\kappa') \end{cases} \tag{5}$$

The corresponding minimum cutting thickness profile y_{min1} can be expressed as

$$y_{\min 1} = \begin{cases} (r_\varepsilon - h_{\mathrm{Dmin}})\, y_1 / r_\varepsilon \; ; (r_\varepsilon + f_z) \geq x > (f_z - r_\varepsilon \sin\kappa') \\ y_1 - h_{\mathrm{Dmin}} \cos\kappa' \qquad ; x \leq (f_z - r_\varepsilon \sin\kappa') \end{cases} \tag{6}$$

Then, for the subsequent i tooth pass, the cutter profile y_i can be expressed as

$$y_i = \begin{cases} \sqrt{r_\varepsilon^2 - (x - if_z)^2} & ; (r_\varepsilon + if_z) \geq x > (if_z - r_\varepsilon \sin\kappa') \\ r_\varepsilon \cos\kappa' + [(x - if_z) + r_\varepsilon \sin\kappa']\tan\kappa' ; x \leq (if_z - r_\varepsilon \sin\kappa') \end{cases} \tag{7}$$

The corresponding minimum cutting thickness profile y_{mini} can be expressed as

$$y_{\min i} = \begin{cases} (r_\varepsilon - h_{\mathrm{Dmin}})\, y_i / r_\varepsilon \; ; (r_\varepsilon + if_z) \geq x > (if_z - r_\varepsilon \sin\kappa') \\ y_i - h_{\mathrm{Dmin}} \cos\kappa' \qquad ; x \leq (if_z - r_\varepsilon \sin\kappa') \end{cases} \tag{8}$$

Then, with each pass of the tooth, the surface profile along the centerline of the slot floor can be computed through combining the old computed surface profile.

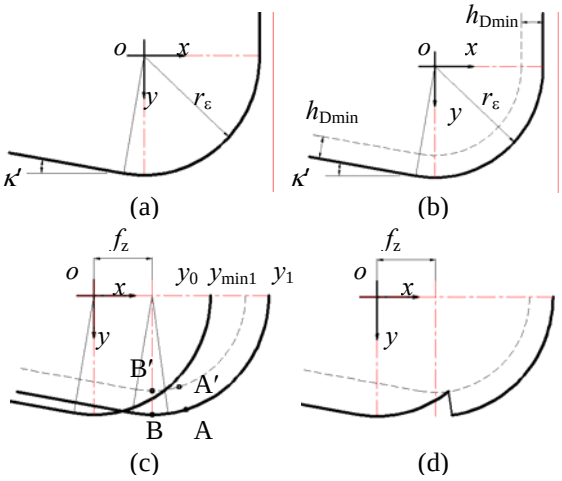

Fig.2 Schematic illustration of the surface generation along the slot floor centerline

For example, the case for the first tooth pass is shown in Fig.2(c). At point A, the corresponding minimum cutting thickness point is A', the minimum cutting thickness is exceeded, and then the chips are formed and the surface profile is updated to include point A. However, at point B, the corresponding minimum cutting thickness point is B', the cutting thickness is less than the minimum cutting thickness, and then no

chip is formed and the surface profile is not updated. Fig.2(d) shows generated surface profile after the first tooth pass. With the repeat of this process, the surface profile along the centerline of the slot floor is generated.

2.2 2D simulation of surface topography

After the minimum cutting thickness is determined, the above model can be used to simulate the surface profile along the centerline of the slot floor. Once the surface profile is generated, the arithmetic surface roughness R_a can be computed. The surface topography 2D simulation program is developed using MATLAB and the flow chart is shown in Fig.3, n is the number of the tooth pass.

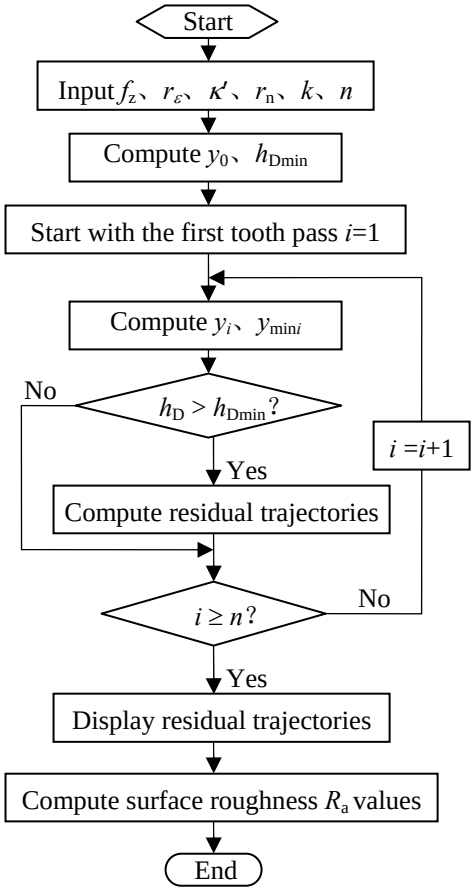

Fig.3 Flow chart of the surface topography simulation

A tungsten carbide 2-fluted flat end milling cutter of diameter 500 μm is used for the subsequent experiments. The cutting edge radius, the nose radius and the concave angle are estimated using SEM to be 2μm, 2μm and 5°, respectively. Suppose that k is 0.3, and then the simulated surface topography with the feed per tooth of 2μm and 0.5μm and the computed surface roughness R_a values are shown in Fig.4. For the feed per tooth of 2μm, the periods of the saw-toothed surface profile is equal to the feed per tooth 2μm. For the feed per tooth of 0.5μm, the periods of the saw-toothed surface profile is 1μm, not equal to the feed per tooth. This indicates that no chip is formed with each pass of the tooth for a smaller feed per tooth due to the minimum cutting thickness effect. Instead, the tooth can rotate several times without performing any cutting. The chips are formed when the minimum cutting thickness is exceeded [4].

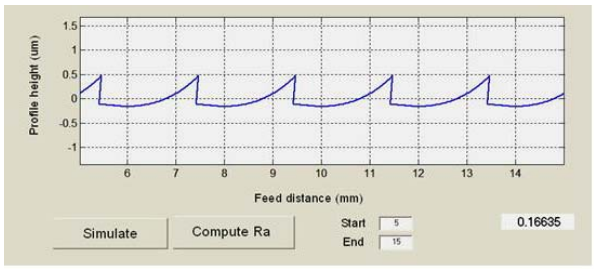

(a) f_z = 2 μm

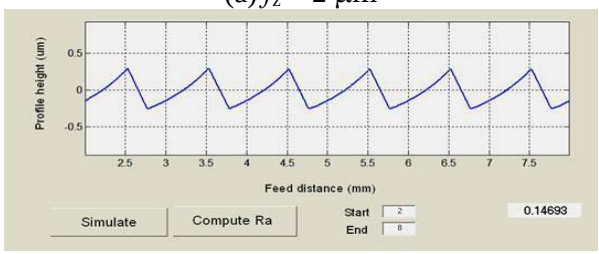

(b) f_z = 0.5 μm

Fig.4 Simulation of the surface topography along the slot floor centerline

3 Micro-milling Experiments

3.1 Experimental conditions

Experiments are performed on the developed miniaturized machine tool, as shown in Fig.5. This is a horizontal 3-axis numerical control milling machine tool. The overall size of the machine tool is 300×150×165 mm. The spindle speed is controlled by changing the air pressure, and its maximum is 150000r/min. The feed system is composed of three precision linear tables with crossed roller bearing linear guides. The 3-axis table, whose travel range is 30×30×25 mm, is stacked on the workpiece side of the machine tool and driven by a piezoelectricity ceramics ultrasonic motor, respectively, while the cutter is clamped on the spindle and held in a stationary location during milling. The feed system resolution is 0.1 μm. Each axis has a resolution 0.05μm optical linear encoder used to provide positioning feed-back.

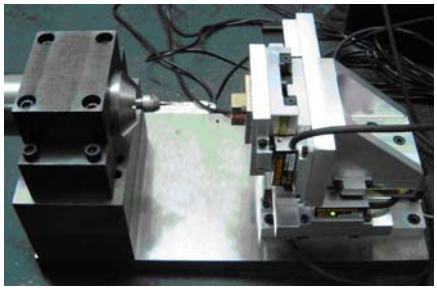

Fig.5 Miniaturized machine tool

In the experiments, the workpiece material is AL6061, and the machining operation is slot milling with dry cutting. The axial depth of cut a_p and the cutting speed v_c, are constant at 50 μm and 80 m/min, respectively. The feed per tooth f_z, is varied from 0.125μm, 0.25μm, 0.5μm, 1μm, 2μm, 3μm to 4μm, respectively. For each feed tested, three grooves of length 7 mm are cut, and surface roughness is measured by a Form Talysurf (S4C) surface profile measuring system along the centerline of a slot floor. Fig.6 shows an example of surface profile measurement at the feed per tooth of 3 μm.

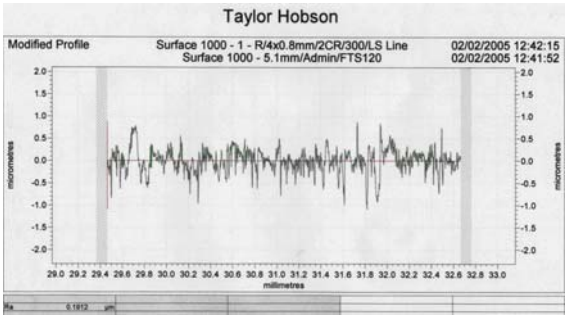

Fig.6 Surface profile along the centerline of a slot floor and its surface roughness R_a values

3.2 Experimental results and analysis

The average of measured surface roughness R_a values for the same feed tested and the corresponding computed surface roughness R_a values using the above model are shown in Fig.7. Both the results show that the surface roughness values is significantly affected by the feed, and the surface roughness values increase as the feed per tooth is reduced to a certain value, namely the existence of an optimal feed that will produce the smallest surface roughness values. Obviously, this is different from the trend of the surface roughness values with reducing feed observed in conventional milling process. Fig.7 indicates that the proposed surface generation model can reasonably describe and explain the trend of the surface roughness values with the varying feed in micro-milling process, and also indicates that the minimum cutting thickness has a significant influence on the achievable surface roughness in micro-milling process.

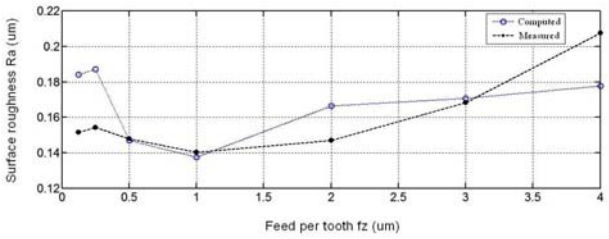

Fig.7 Computed and measured surface roughness R_a values

Generally, the factors contributing to the surface roughness include the geometry and the instability in machining process. The former is mostly the height of the residual area generated based on the geometry of the cutter and process parameters, and the later includes vibration, deflection, chatter, and built-up edge formation, etc. In conventional milling process, the residual area is generated based on the concave angle, the nose radius and the feed, and then the surface roughness values will exhibit the conventional trend of increasing roughness with increasing feed. In micro-milling process, process parameters are often comparable to the geometry of the cutter, due to the existence of the minimum cutting thickness, and then the residual area is generated based on the combined effects of the geometry of the cutter, process parameters, and the minimum cutting thickness. Especially for a smaller feed per tooth, when the minimum cutting thickness is not exceeded, the cutter rotates several times without removing any material, and the consequent residual area is larger than the residual area generated based solely on the geometry of the cutter and process parameters. As a result of the combined effects, an optimal feed exists to produce the smallest surface roughness value. It is obvious that the effect of the minimum cutting thickness is dominant at smaller feed in micro-milling process. Moreover, the rubbing and the plowing of the workpiece material under the cutting edge will affect the chip formation [4], and will affect the machined surface qualities.

4 Factors affecting surface roughness in micro-milling

As the size of a cutter decreases, its geometry cannot be improved proportionally because of limitations in the cutter fabrication processes. Using the above

model, the influence of the cutter geometry on the surface roughness in micro-milling can be analyzed.

4.1 Effects of minimum cutting thickness and the cutting edge radius

Suppose that the cutting edge radius r_n=2μm, the nose radius r_ε=2μm, the concave angle κ'=10°, and then the surface roughness R_a values as a function of the feed per tooth in terms of different ratios k as expressed in equation (2) are shown in Fig.8. It is found that the surface roughness values are strongly affected by the ratio k.

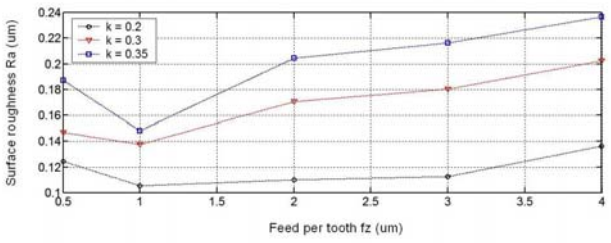

Fig.8 Effect of the ratio k

Suppose that the ratio k=0.3, the nose radius r_ε=2μm, the concave angle κ'=10°, and then the surface roughness R_a values as a function of the feed per tooth in terms of different cutting edge radius r_n are shown in Fig.9. It is found that the surface roughness generated by a cutter with bigger cutting edge radius is much larger than that generated by a cutter with smaller cutting edge radius and the optimal feed that will produce the smallest surface roughness value is increasing with the increasing cutting edge radius.

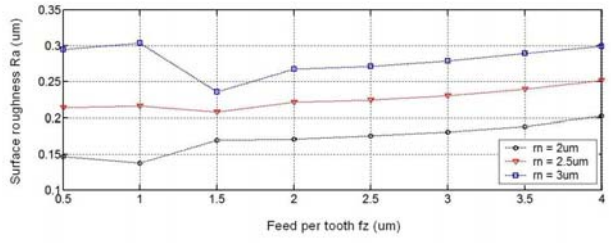

Fig.9 Effect of the cutting edge radius

Clearly, the machined surface roughness is significantly affected by the cutting edge radius and the feed. Combining Fig.8 and Fig.9, it is found that the surface generation in micro-milling process is strongly affected by the cutting edge radius and the feed per tooth through the minimum cutting thickness.

4.2 Effect of the concave angle

Suppose that the ratio k=0.3, the cutting edge radius r_n=2μm, the nose radius r_ε=2μm, and then the surface roughness R_a values as a function of the feed per tooth in terms of different concave angle κ' are shown in Fig.10. It is found that the effect of the concave angle κ' on the surface roughness is insignificant, because of the residual area generated by the motion trajectories of the nose arc cutting edge at a lower feed. When the feed is increased, an increase in the concave angle increases the surface roughness, due to the residual area generated by the motion trajectories of the end cutting edge and the nose arc cutting edge. But a too smaller concave angle will increase the wear of the end cutting edge. As a result, the surface roughness values will be increased instead.

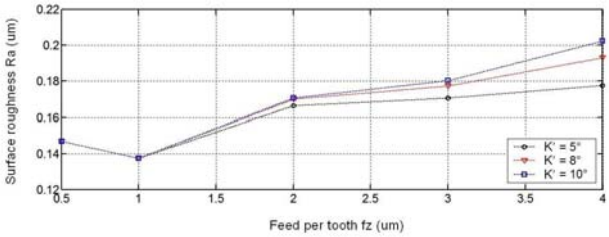

Fig.10 Effect of the concave angle

4.3 Effect of the nose radius

Suppose that the ratio k=0.3, the cutting edge radius r_n=2μm, the concave angle κ'=10°, and then the surface roughness R_a values as a function of the feed per tooth in terms of different nose radius r_ε are shown in Fig.11. It is found that neither a smaller nose radius nor a bigger one will produce the smallest surface roughness values, namely an appropriate nose radius based on the feed exists.

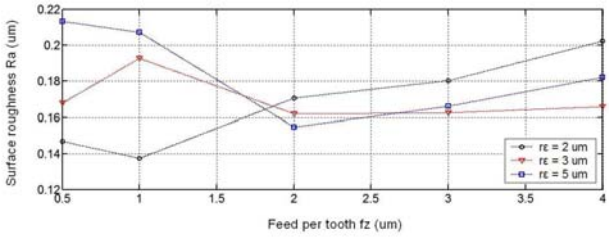

Fig.11 Effect of the nose radius

5 Conclusion

The main conclusions can be drawn as follows:
(1) A model of surface generation 2D simulation based on the minimum cutting thickness is proposed.

Comparison between the computed and the measured surface roughness values indicates that this model can reasonably describe and explain the observed behavior in micro-milling process.

(2) In micro-milling process, when the feed per tooth is reduced to a certain value, the surface roughness values start to increase, namely the existence of an optimal feed that will produce the smallest surface roughness values.

(3) In micro-milling process, the existence of the minimum cutting thickness has a significant influence on the achievable surface roughness values. The existence of the optimal feed is due to the combined effects of the geometry of the cutter and the feed, and the minimum cutting thickness effect. The surface generation in micro-milling process is strongly affected by the combined effects.

Acknowledgement

This paper was partially supported by a grant from the Harbin Institute of Technology (Project No.: HIT.2002.25) and a grant from the Hong Kong Innovation and Technology Commission (Grant No.: ITS/001/05).

References:

[1] B.N. Damazo, M.A. Davies, B.S. Dutterer, M.D. Kennedy, A Summary of Micro-milling Studies, *Proceeding of 1st International Conference and General Meeting of EUSPEN*, Bremen, Germany, 1999, pp. 322-324.

[2] M. Takacs, B. Vero, I. Meszaros, Micromilling of Metallic Materials, *Journal of Materials Processing Technology*, Vol.138, 2003, pp. 152-155.

[3] H. Weule, V. Huntrup, H. Tritschler, Micro-cutting of Steel to Meet New Requirements in Miniaturization, *Annals of the CIRP*, Vol.50, 2001, pp. 61-64.

[4] C.J. Kim, M. Bono, J. Ni, Experimental Analysis of Chip Formation in Micro-milling, *Transaction of NAMRI/SME*, Vol.XXX, 2002, pp. 247-254.

[5] S.N. Melkote, A.R. Thangaraj, An Enhanced End Milling Surface Texture Model Including the Effects of Radial Rake and Primary Relief Angles, *ASME Journal of Engineering for Industry*, Vol.116, 1994, pp. 166-174.

[6] A.P. Xu, Y.X. Qu, W.M. Li, D.W. Zhang, T. Huang, Generalized Simulation Model for Milled Surface Topography – Application to Peripheral Milling, *Chinese Journal of Mechanical Engineering,* Vol.14, No.2, 2001, pp. 121-126.

[7] N. Ikawa, S. Shimada, R. Donaldson, Chip Morphology and Minimum Thickness of Cut in Micromachining, *JSPE*, Vol.5904, 1993, pp. 673-679.

[8] Z. J. Yuan, M. Zhou, S. Dong. Effect of Diamond Tool Sharpness on Minimum Cutting Thickness and Cutting Surface Integrity in Ultraprecision Machining. *Journal of Materials Processing Technology*, Vol.62, 1996, pp. 327-330

[9] M.E. Martellotti, An Analysis of the Milling Process, *Transactions of ASME*, Vol.63, 1941, pp. 677-700.